Journal of Pharmaceutical and Biomedical Analysis 266 (2025) 117081

Contents lists available at ScienceDirect

Journal of Pharmaceutical and Biomedical Analysis

journal homepage: www.journals.elsevier.com/journal-of-pharmaceutical-and-biomedical-analysis

Determining carbon-carbon double bond position of unsaturated glycerophospholipids in human plasma NIST® SRM® 1950 by electron impact excitation of ions from organics-tandem mass spectrometry (EIEIO-MS/MS)

Sara Martínez [a], Ana Gradillas [a], Hana Cermakova [a], Michael Witting [b,c,*], Coral Barbas [a,**]

[a] Centro de Metabolómica y Bioanálisis (CEMBIO), Facultad de Farmacia, Universidad San Pablo-CEU, CEU Universities, Urbanización Montepríncipe, Boadilla del Monte, Madrid 28660, Spain
[b] Metabolomics and Proteomics Core, Helmholtz Zentrum München, Neuherberg, Germany
[c] Chair of Analytical Food Chemistry, TUM School of Life Sciences, Technical University of Munich, Freising-Weihenstephan, Germany

ARTICLE INFO

Keywords:
Electron-induced dissociation (EID)
Electron impact excitation of ions from organics (EIEIO)
MS/MS fragmentation
NIST SRM 1950
Double bond position
Lipidomics
Lipid annotation

ABSTRACT

Understanding the structural diversity and biological functions of unsaturated fatty acyl chains (FAC) esterified in complex lipids –such as glycerolipids (GL), glycerophospholipids (GP) or sphingolipids (SP)– requires precise knowledge of the degree of unsaturation, location, and geometrical isomerism of the carbon-carbon double bonds (C=C). However, the complex isomeric nature of lipids, combined with the inherent limitations of conventional tandem mass spectrometry (MS/MS) in structural elucidation, remains a major challenge in accurate C=C elucidation. To overcome this, advanced MS/MS strategies, such as electron impact excitation of ions from organics (EIEIO) have emerged, generating diagnostic fragment ions that enable unambiguous C=C localization. In the present study, we conducted a qualitative structural analysis of the C=C positions in esterified FAC of GP present in NIST® Human Plasma Standard Reference Material, SRM 1950, employing RP-UHPLC-ESI(+)-EIEIO-QTOF-MS/MS. Interpretation of ESI(+)-EIEIO-MS/MS spectra enabled C=C determination in 120 unsaturated GP, revealing a predominance of ω-6 and ω-3 FAC. These results offer new insights into the FAC distribution of this reference material, enhancing the structural annotation confidence level. By integrating such detailed molecular information, EIEIO-MS/MS proves to be a powerful approach for in-depth lipid structural elucidation in complex biological matrices, thereby contributing to methodological advancements and supporting its future application in translational lipidomics.

1. Introduction

The number and precise location of carbon-carbon double bonds (C=C) within fatty acyl chains (FAC), as well as their geometrical isomerism, are essential structural attributes that significantly influence their biological function, impacting membrane fluidity, signaling pathways and lipid-protein interactions [1,2]. Comprehensive analysis of the FAC composition and unambiguous C=C structural elucidation is therefore crucial in mass spectrometry (MS)-based lipidomic studies, as it provides key insights into underlying biochemical pathways and lipid metabolism [3].

However, despite extensive research, identifying and differentiating FAC regio- and stereochemical variations remains a major challenge, due to the large and complex combinatorial space of lipids, which leads to numerous isobaric and isomeric structures even within single lipid classes [4]. To address this challenge, separation techniques such as liquid chromatography (LC) coupled with electrospray ionization (ESI) and high-resolution mass spectrometry (HRMS) are widely used, utilizing MS1 data to resolve isobaric overlaps, and tandem MS (MS/MS) for the structural elucidation of isomeric species [5].

The vast majority of lipidomic MS/MS analyses have relied on low-energy collision-induced dissociation (CID), due to its accessibility and widespread application in metabolomics and lipidomics studies [6]. However, CID-based structural analysis alone has often been insufficient

* Corresponding author at: Metabolomics and Proteomics Core, Helmholtz Zentrum München, Neuherberg, Germany.
** Corresponding author.
E-mail addresses: michael.witting@helmholtz-munich.de (M. Witting), cbarbas@ceu.es (C. Barbas).

https://doi.org/10.1016/j.jpba.2025.117081
Received 30 May 2025; Received in revised form 22 July 2025; Accepted 23 July 2025
Available online 24 July 2025

to generate diagnostic fragment ions for C=C position determination. To cover this limitation, sophisticated but complex chemical and photochemical solution-phase derivatization reactions, and gas-phase reactions have been coupled to CID, enabling C=C localization [7,8] (Fig. 1A).

In recent years, advancements in instrumentation have led to the development of enhanced MS/MS methods that enable direct C=C cleavage without needing previous modifications offering improved resolution for detailed lipid structural characterization [7] (Fig. 1B, C). Among these, after ionization dissociation methods, including photon-, radical- and electron-based fragmentations, (Fig. 1C), have expanded the capabilities of lipid analysis, addressing key limitations associated with traditional low-energy CID-MS/MS-based workflows.

Of particular interest has been the use of electron-induced dissociation (EID), which has emerged as a powerful technique for structural elucidation of biological molecules, offering unique fragmentation pathways not achievable through other gas-phase dissociation methods [9]. Within EID, several dissociation methods exist, primarily distinguished by the applied electron kinetic energy (eKE) –which ranges from 5 to 50 eV– and the nature of the precursor molecules [9] (Fig. 1C). In all instances, fragmentation is driven by the interaction of positively charged ions with an electron beam, resulting in high-energy, radical--directed dissociation pathways.

For single-charged small molecules, such as lipids, electron impact excitation of ions from organics (EIEIO) is typically employed, utilizing a eKE range of 5–16 eV [10] (Fig. 1C). Unlike other advanced-MS/MS techniques limited to C=C position-specific cleavage, EIEIO induces extensive molecular dissociation, producing a wide array of fragments that provide multilevel structural information, such as head group, backbone, FAC composition, *sn*-regioisomerism, C=C position and/or geometrical isomerism [7]. Additionally, EIEIO has demonstrated potential for localizing functional groups (*e.g.*, those in oxidized lipids), as well as structural features like branched-chain substitutions.

To date, EIEIO-MS/MS has been applied in lipidomics using two commercial MS platforms. Initial studies –between 2015 and 2018– employed a modified SCIEX TripleTOF 5600 system with a branched radio frequency ion trap to determine C=C positions in esterified FAC within glycerolipids (GL), glycerophospholipids (GP), and sphingolipids (SP), using authentic lipid standards and complex commercial mixtures [10–14]. More recently, –between 2023 and 2025– the SCIEX ZenoTOF 7600 system has been used to determine C=C positions in triglycerides from animal and human samples [15], and to develop an LC-EIEIO-MS/MS-based method for *de novo* lipid annotation up to C=C localization [16]. Among these, only one study has assessed *cis/trans* isomerism using standards and ruminant samples [10] (Supplemental Table S1).

In addition, computational tools such as MS-DIAL 5, developed using the SCIEX ZenoTOF 7600 system together with authentic standards and biological samples, are currently available to support C=C annotation efforts [17]. Nevertheless, extensive and expert-driven manual curation remains essential for refining results.

Recently, we developed an LC-MS lipidomic database using the NIST® Human Plasma Standard Reference Material, SRM 1950, in which 592 lipid species across 20 subclasses were accurately identified [18]. Lipid characterization was performed using an ESI (+/–)-CID-MS/MS strategy, followed by a comprehensive annotation workflow, that ensured broad coverage, structural accuracy and annotation consistency [18]. Among the lipid classes, GP represented the

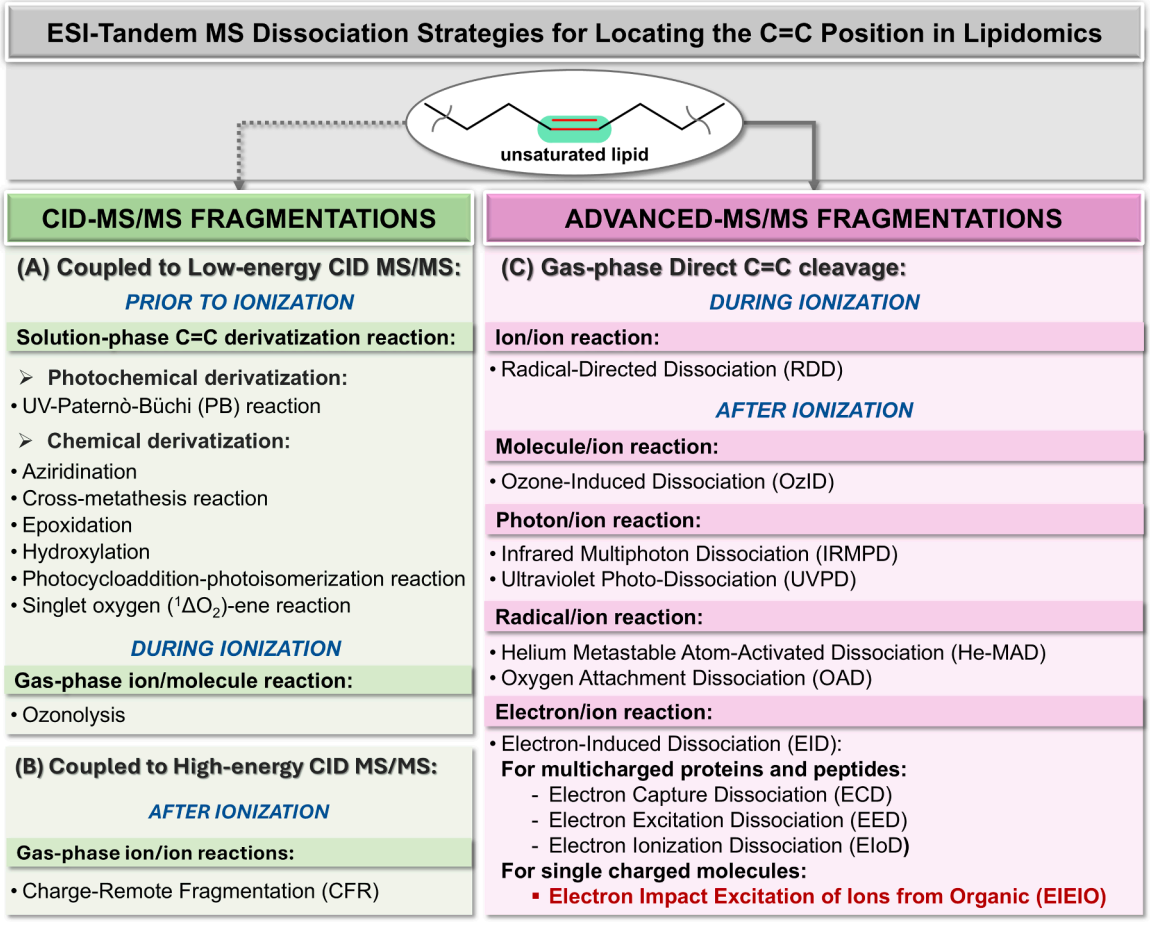

Fig. 1. Overview of selected ESI-Tandem MS dissociation strategies for locating C=C position in lipidomics. Highlighted in red is the EIEIO-MS/MS fragmentation mode used in the present study.

most abundant group, accounting for 48.65 % of the lipidome. While our approach provided detailed structural resolution, it was not fully complete as far as C=C location is concerned. Therefore, the use of advanced MS/MS strategies, which offer greater versatility and are particularly valuable for the determination of C=C positions, is essential to achieve more detailed structural information.

Although EIEIO-MS/MS has been previously applied in lipidomics, no comprehensive annotation of C=C position in SRM 1950 has been reported yet. Furthermore, while other derivatization-based strategies (Fig. 1A) attempted C=C localization in SRM 1950, these studies have typically used it as a quality control material, without generating a curated, openly accessible dataset. Thus, the structural information of unsaturated lipids remains limited.

Here, we present the first systematic characterization of C=C positions in unsaturated esterified FAC within GP from SRM 1950, building upon our LC-MS lipidomic database [18]. To accomplish this, a qualitative workflow based on RP-UHPLC-ESI(+)-EIEIO-MS/MS analysis was followed (Supplemental Fig. S1), incorporating authentic endogenous lipid standards to support and confirm spectral interpretation. These results offer new insights into the FAC distribution of this reference material, by enhancing the structural annotation confidence level.

Moreover, complementary RP-UHPLC-ESI(+/–)-CID-MS/MS analyses were performed to further identify FAC composition and *sn*-position of lipid species previously annotated at the sum composition level [18], taking advantage of the increased MS/MS sensitivity provided by the instrumentation used [19].

To the best of our knowledge, this study provides the most advanced structural characterization of unsaturated GP in SRM 1950 to date, expanding the utility of this reference material by integrating C=C positional detail and serving as a resource-driven contribution that bridges analytical innovation with biological insights into lipid-mediated inflammation in the material.

2. Materials and methods

2.1. Analytical standards, reagents and sample

LC-MS grade water, methanol (MeOH), acetonitrile (ACN), isopropanol (IPA) and *tert*-butyl methyl ether (MTBE) were purchased from Merck KGaA (Darmstadt, Germany). Ammonium fluoride (NH_4F) (ACS reagent, ≥ 98 %), ammonium hydroxide solution (ACS reagent, 28.0–30.0 % NH_3 basis), C17-sphinganine and deuterated palmitic acid-(d31) were purchased from Sigma-Aldrich (Steinheim, Germany). Acetic acid (≥ 99 %) was obtained from Fisher Scientific (Waltham, MA, USA). SPLASH® LIPIDOMIX® Mass Spec Standard, a stable mixture of 14 deuterium-labeled lipids, and 23 authentic chemical lipid standards –including both saturated [PC(14:0/14:0), PE(14:0/14:0), PE(15:0/15:0), PC(16:0/16:0), PE(16:0/16:0), PC(16:0/18:0), PE(17:0/17:0), PC(18:0/18:0), PC(20:0/20:0)], and unsaturated species [PC(16:0/18:1(9Z)), PE(16:0/18:1(9Z)), PC(16:0/18:2(9Z,12Z)), PE(16:0/18:2(9Z,12Z)), PC(16:0/20:4(5Z,8Z,11Z,14Z)), PE(16:0/20:4(5Z,8Z,11Z,14Z)), PC(16:0/22:6(4Z,7Z,10Z,13Z,16Z,19Z)), PE(16:0/22:6(4Z,7Z,10Z,13Z,16Z,19Z)), PE(18:0/18:1(9Z)), PC(18:0/20:4(5Z,8Z,11Z,14Z)), PE(18:0/20:4(5Z,8Z,11Z,14Z)), PC(18:0/22:6(4Z,7Z,10Z,13Z,16Z,19Z)), PE(18:0/22:6(4Z,7Z,10Z,13Z,16Z,19Z)), PC(18:1(9Z)/16:0)]– were purchased from Avanti Polar Lipids, Inc (Alabaster, AL, USA). Detailed information about the endogenous lipid standards is given in Supplemental Table S2.

2.2. Human plasma sample

National Institute of Standards and Technology (NIST®) Standard Reference material (SRM®) 1950 Metabolites in Frozen Human Plasma was purchased from Sigma-Aldrich (Steinheim, Germany)

2.3. Lipid standard mixture preparation

Six lipid standard mixtures –containing the 23 authentic chemical lipid standards– were prepared in MeOH to support spectra interpretation, structural elucidation and annotation validation. Lipid standard mixtures were carefully designed to avoid isomeric and isobaric overlaps, with each standard maintained at a concentration of 10 ppm to ensure sufficient fragment ion intensity for accurate method optimization and spectral interpretation. The composition of each lipid standard mixture is detailed in Supplemental Table S2.

2.4. Sample preparation: lipid extraction

Lipids from the SRM 1950 human plasma sample were extracted following an all-in-one single-phase lipid extraction method based on a monophasic solvent mixture composed of MeOH/MTBE (1:1, v/v) to cover the isolation of polar and non-polar lipids [20]. A detailed description of the lipid extraction method is given in the Supporting Information.

2.5. Analytical conditions

Three replicates of the SRM 1950 lipid extract and the authentic endogenous lipid standard mixtures were analyzed using an Agilent 1290 Infinity II Bio UHPLC system (Agilent Technologies, Santa Clara, CA, USA) coupled to a SCIEX ZenoTOF 7600 QTOF Mass Spectrometer (SCIEX, Toronto, Canada) equipped with the Turbo V Ion Source with Twin Sprayer Electrospray Ionization (ESI) probe enabling both EIEIO and CID fragmentation modes.

Quality management (QM) was consistently maintained throughout the pre-analysis, analysis, and post-analysis phases. To ensure robust QM, we followed the Metabolomics Quality Assurance and Quality Control Consortium guidelines (mQACC) [21].

2.5.1. Reverse-phase liquid chromatography

For the RP-UHPLC analysis, an optimized method already reported in previous lipidomic studies was implemented [18,22]. A detailed description of the method is given in the Supporting Information.

2.5.2. Mass spectrometry

All experiments were performed using the ZenoTOF 7600 system with ESI-EID-QTOF-MS configuration, using both ESI(+)-EIEIO and ESI(+/–)-CID fragmentation modes (Supplemental Fig. S2A and S2B). Both EIEIO and CID were separately employed, with all experiments conducted in automated data-dependent acquisition (DDA) mode. The ESI source was operating in all cases with the following parameters: source temperature, 500 °C; curtain gas, 40 psi; ion source gas 1 (GS1), 60 psi; ion source gas 2 (GS2), 60 psi; CAD gas, 7 psi. Additional MS experimental parameters are provided in Supplemental Fig. S2C.

For DDA experiments different inclusion lists –one for each targeted lipid subclass comprising only unsaturated lipid species with abundances over 10^4 in the reported database [18]– were used. These lists, containing information on the selected lipid species and mass-to-charge ratio (m/z) of the $[M+H]^+$ adduct ion, guaranteed the collection of high-resolution product ion spectra. An "MS quick check" tune was performed in both polarities before any analysis to ensure instrument calibration. In addition, prior to EIEIO measurements, an "EAD background reduction" was run to help clean the EID cell.

Raw acquisition and data processing were performed using the Explore module of SCIEX OS software (*v*. 3.3.0, SCIEX, Toronto, Canada) to structurally elucidate lipid species from EIEIO-MS/MS and CID-MS/MS based ion spectra.

2.6. Nomenclature

For lipid category classification and nomenclature, we adhered to the

classification system established by LIPID MAPS [23]. When describing FAC, common names were used when available, if not, semi-systematic names were employed.

The nomenclature of the C=C position followed the analogous "ω" notation for general families or series, and "n" notation for specific FAC, in line with IUPAC recommendations. Geometrical isomers (*cis* (*Z*)/*trans* (*E*)) were annotated using delta "Δ" nomenclature.

3. Results and discussion

After running the SRM 1950 human plasma sample, a general comparison of the Total Ion Chromatograms (TIC) in ESI(+) (Fig. 2) between the SRM 1950 sample analyzed in the current study and for the construction of the SRM 1950 lipid database [18] revealed a high degree of consistency, exhibiting nearly identical lipid profiles and ensuring comprehensive lipid coverage across the entire polarity spectrum (Fig. 2). Additionally, two critical parameters were assessed across the runs: mass accuracy and retention time (RT) deviation. Mass accuracy was consistently maintained; however, despite using the same chromatographic method, an expected RT shift was detected across all subclasses (Fig. 2). This shift, which varied depending on the gradient composition of the mobile phases during the chromatographic separation (Fig. 2 and Supplemental Table S3), was potentially attributed to pipeline variations (*e.g.,* inner diameter and length) between LC-MS instruments.

To estimate the expected RT of the lipids of interest without requiring additional manual inspection, selected endogenous lipid species, along with the deuterium-labeled lipid species from SPLASH® LIPIDOMIX® were used, taking our lipidomic database [18] as a reference template (Supplemental Table S3). This enabled fast identification of the targeted lipid species and validated the applicability of the database across different instruments. Annotation and RT were further confirmed in all cases by examining EIEIO and CID spectra individually. Extracted ion chromatograms (EIC) displaying RT of the detected SPLASH® LIPIDOMIX® deuterium-labeled lipid species in ESI(+) are shown in Supplemental Fig. S3.

3.1. Structural elucidation of the RP-UHPLC-ESI(+)-EIEIO-MS/MS spectra enables C=C position determination

Starting from our SRM 1950 lipidomic database, which includes annotations up to the FAC [18], SRM 1950 human plasma sample was now analyzed using RP-UHPLC-ESI(+)-EIEIO-MS/MS to qualitatively determine, after manual MS/MS interpretation, C=C positions in unsaturated GP and sphingomyelins (SM) included in the database. Besides C=C position information, EIEIO-MS/MS spectra displayed near-complete structural information in a single experiment, producing a comprehensive fragmentation pattern that provided information of specific head group subclass, backbone, regioisomer arrangement of the FAC (*sn*-1 position) and specific cleavages corresponding to the FAC length and C=C position, (Supplemental Fig. S4), therefore allowing in-depth structural elucidation.

PC, PE and SM identification were carried out exclusively using the predominant protonated adduct $[M+H]^+$, as previously reported for these specific lipid subclasses [10–12]. For GP, identification began with the assignment of the head group. This was achieved by detecting the diagnostic fragment ion *m/z* 184.0730 in LPC, PC, and PC (O/P) (Fig. 3), and a characteristic neutral loss of *m/z* 141.0191 from the precursor ion in LPE, PE and PE (O/P) species (Supplemental Fig. S5) [24]. Subsequently, glycerol backbone-based lipids displayed two characteristic fragment ions corresponding, for LPC, PC and PC (O/P) to '*C*-type' (*m/z* 224.1053) and '*O*-type' (*m/z* 226.0845) cleavages (Fig. 3). For LPE, PE and PE (O/P) the respective '*C*-type' and '*O*-type' fragments were observed at *m/z* 182.0582 and *m/z* 184.0375 respectively (Supplemental Fig. S5) [14,24,25]. Finally, the determination of the *sn*-position and FAC composition was based on a characteristic radical cleavage at the C_1-C_2 bond of the glycerol backbone. This cleavage generates a key diagnostic ion that allows the distinction between *sn*-1 and *sn*-2 FAC. Additional fragments, such as those from *sn*-1 C_1-O and O-(C_1=O) cleavages, further support lipid structure identification. Spectra were interpreted according to established guidelines for GP [11, 14].

In the case of SM, the head group was equally identified by the presence of the diagnostic fragment ion at *m/z* 184.0730. SM backbone characterization proceeded with the identification of the sphingoid-specific '*N*-type' cleavage (*m/z* 225.0975) (Supplemental Fig. S6).

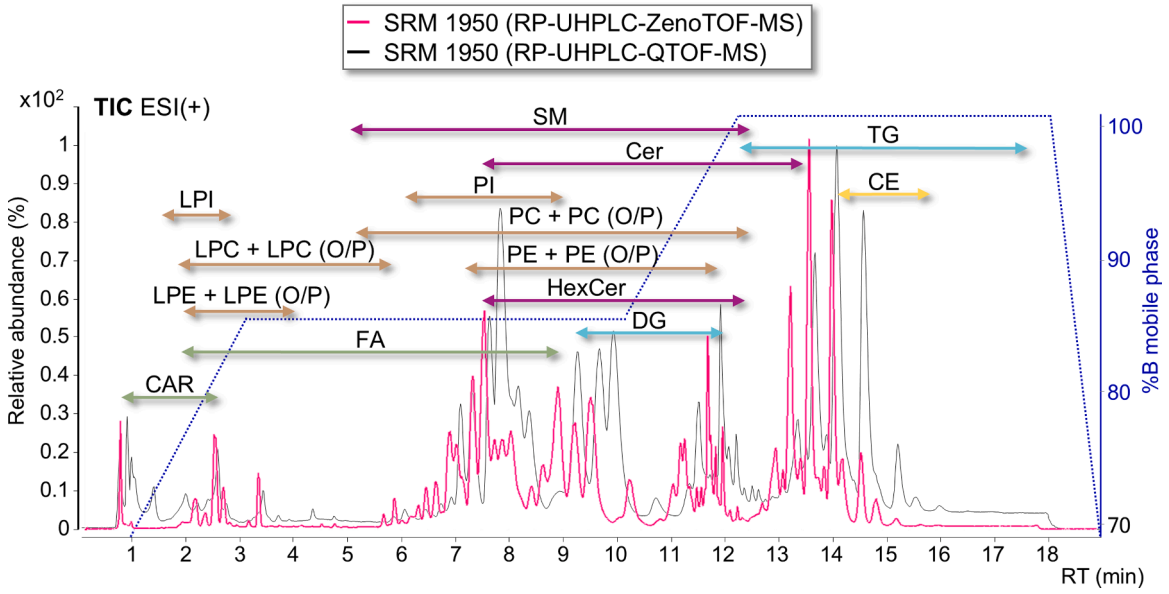

Fig. 2. Chromatographic Lipid Profile. Overlay of the Total Ion Chromatogram (TIC) in ESI(+) of SRM 1950 measured in this analysis (TIC in pink) –using the Agilent 1290 Infinity II Bio UHPLC coupled to the SCIEX ZenoTOF 7600 QTOF-MS– and for the construction of the lipid database (TIC in black) –utilizing the Agilent 1290 Infinity II UHPLC coupled to an Agilent 6545 QTOF-MS– [18], and mobile phase composition over the chromatographic separation method (in blue): I = isocratic, G = gradient. I1 [0–1 min], G1 [1–3.50 min], I2 [3.50–10 min], G2 [10–11 min], I3 [11–17.10 min] and G3 [17.10–19 min].

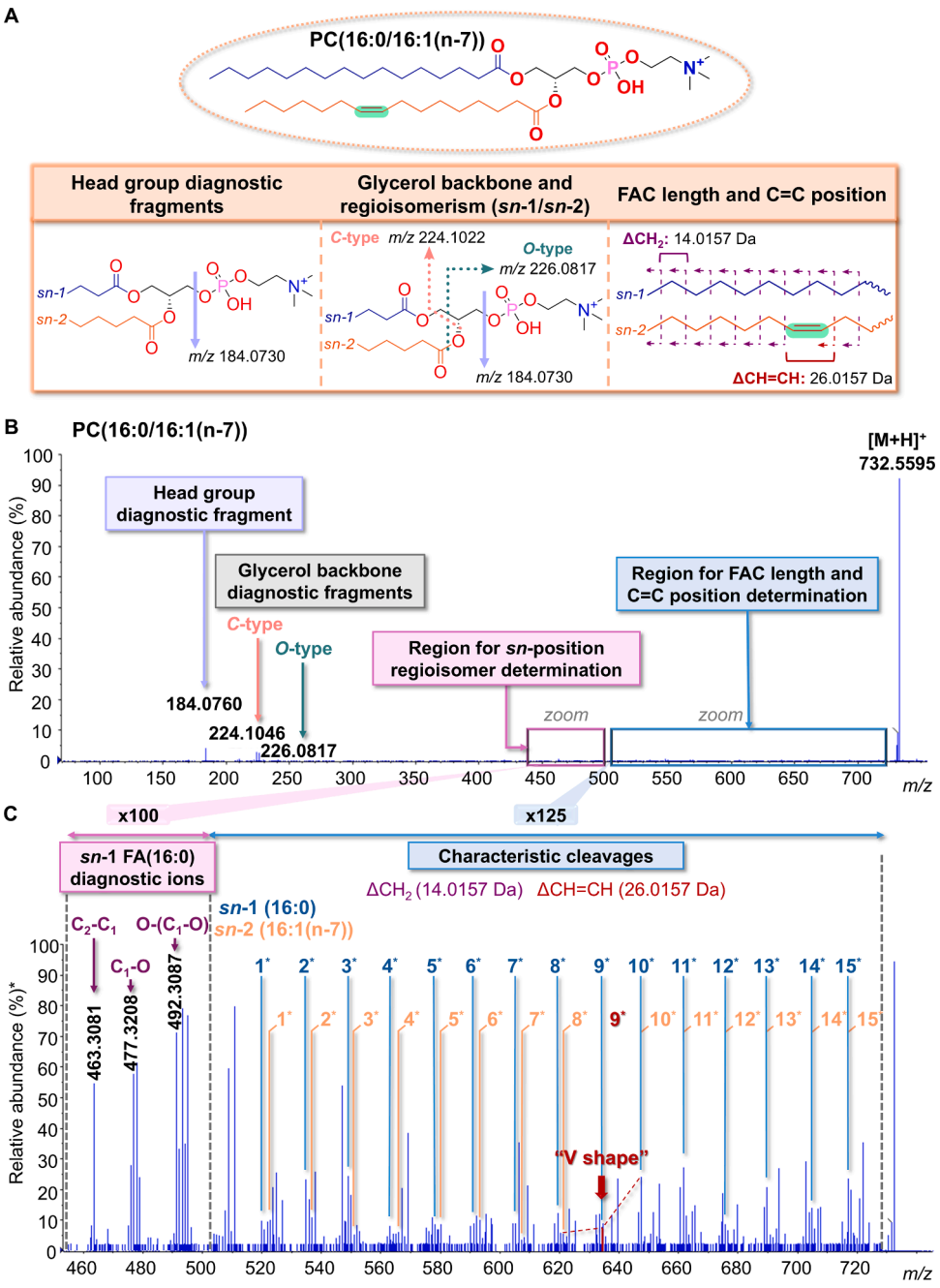

Fig. 3. Localization of C=C position in PC(16:0/16:1(n-7)) using ESI(+)-EIEIO-MS/MS. (A) Expected fragment ions for LPC, PC and PC (O/P). (B) ESI(+)-EIEIO spectrum. (C) Zoomed ESI(+)-EIEIO-MS/MS spectrum: ion intensity between *m/z* 450 – 500 was amplified 100-fold to identify the fragmentation pattern for *sn*-1 positional regioisomer determination. Ion intensity between *m/z* 500 – 732 was amplified 125-fold for C=C position fragmentation pattern determination. For C=C position, first the formation of a radical fragment occurs, followed by a series of even- and odd-electron fragment ions that provide C=C position information. *Relative abundance refers to the chromatogram without zoom (*i.e.*, a zoom of 100-fold indicates that if represented with relative abundance, the peak intensity will decrease 100 times).

Then, the sphingoid base backbone was determined by detecting an intense radical fragment ion resulting from C_2-C_3 bond cleavage, following previously reported guidelines for SM characterization [14].

For C=C position assignment in all lipid subclasses, first the formation of a radical cation ($[M]^{\bullet+}$), initiated by the loss of a hydrogen atom from the precursor ion $[M+H]^+$ occurs; however, the application of additional energy generates a series of even- and odd-electron second-generation fragment ions between the precursor and the *sn*-1/*sn*-2 diagnostic ions [11]. These fragment ions, although of low intensity (generally < 1 % of base peak) due to limited EIEIO fragmentation efficiency, could be interpreted by zooming into specific regions of the spectra (Fig. 3). In saturated FAC, a continuous series of fragment ions separated by a methylene group (-CH_2-) (14.0157 Da) were detected due to carbon-carbon single bond (C-C) cleavages along the FAC (Fig. 3). For unsaturated FAC, characteristic -CH=CH- cleavages corresponding to 26.0157 Da were produced at each double bond (Fig. 3). Among possible cleavage sites, allylic C-C cleavages were the most favorable. Meanwhile, cleavages at vinylic C-C bonds and at the C=C double bond itself occurred least frequently. This cleavage preference resulted in a characteristic "V-shaped" intensity pattern, facilitating the localization of the C=C [11,25]. Interferences from overlapping -CH=CH- cleavages (26.0157 Da) with the second isotopic peak of two consecutive -CH_2-

Table 1
C═C position in unsaturated esterified fatty acyl chains detected in GP and SM. Abbreviations: FAC, Fatty Acyl Chain.

FAC length	Unsaturation degree	Nomenclature 'n' system	Common name (Abbreviation)
C16	1	C16:1(**n−7**)	Palmitoleic acid
C18	1	C18:1(**n−7**)	Vaccenic acid
	1	C18:1(**n−9**)	Oleic acid (OA)
	2	C18:2(**n−6**,9)	Linoleic acid (LA)
	3	C18:3(**n−3**,6,9)	α-Linolenic acid (ALA)
C20	1	C20:1(**n−9**)	Gonodic acid
	2	C20:2(**n−6**,9)	Dihomolinoleic acid (DLA)
	3	C20:3(**n−6**,9,12)	Dihomo-γ-Linoleic acid (DGLA)
	4	C20:4(**n−6**,9,12,15)	Arachidonic acid (AA)
	5	C20:5(**n−3**,6,9,12,15)	Timnodonic acid (EPA)
C22	1[a]	C22:1(**n−9**)	Erucic acid
	4	C22:4(**n−6**,9,12,15)	Adrenic acid (ADA)
	5	C22:5(**n−6**,9,12,15,18)	Osbond acid (DPA)
	5	C22:5(**n−3**,6,9,12,15)	Clupanodonic acid (DPA)
	6	C22:6(**n−3**,6,9,12,15,18)	Cervonic acid (DHA)
C24	1[a]	C24:1(**n−9**)	Nervonic acid
	2[a]	C24:2(**n−6**,9)	Tetracosadienoic acid

[a]FAC only detected in SM

losses (28.2114 Da) were avoided, as the isolation width used did not include isotopes. A detailed version of how to interpret EIEIO-MS/MS spectra to determine C═C position is shown in Supplemental Fig. S7 and additional examples are provided in Supplemental Fig. S5, S6 and S8.

Given the complexity of the EIEIO-MS/MS spectra, bioinformatic tools such as MZmine [26] and MS-DIAL [17], have been developed to assist C═C positions determination [17,26]. However, this task remains challenging, particularly for lipids containing polyunsaturated FA (PUFA) in complex matrices, as EIEIO generates a high number of fragment ions, sometimes leading to multiple possible annotations for a single lipid species. Consequently, even with computational support, manual curation and expert-driven knowledge is mandatory to ensure accurate interpretation [27].

To facilitate this process, we have developed a customized calculator to determine *sn*-positional regioisomers and the glycerol backbone in GP, the sphingoid backbone in SM, and C═C positions in both lipid classes. Based on the reported characteristic fragments [11,12,14], this tool generates theoretical *m/z* values for expected fragments of a given precursor ion when ionized as protonated adduct $[M+H]^+$. This useful calculator is available as an Excel file in Supplemental Table S4.

To support annotations, selected lipid species were validated against 23 endogenous authentic lipid standards. The evaluation was performed using MS1 and MS/MS scanning modes matching exact *m/z*, RT, and fragmentation pattern, including C═C position fragmentation. Detailed information of the elucidated lipid standards is given in Supplemental Table S5.

As a result, within the GP class, 120 lipid species from a total of 167 unsaturated GP (with known FAC) in the SRM 1950 lipid database were identified up to the C═C position. This represented 71.85 % of the total GP, and included LPC, PC, PC (O/P), LPE, PE and PE (O/P) lipid subclasses (Supplemental Table S6). In addition, among these 120 GP, 97 lipid species were fully characterized, including *sn*-1 and *sn*-2 FAC composition, accounting for over 80 % of the identified lipids. For 23 GP, the C═C position was only determined for *sn*-2 FAC, with 22 of these being PC (O/P) and PE (O/P). This limitation was primarily attributed to two factors related with structural and spectral complexity: (i) the identical *sn*-positional diagnostic fragments of ether GP –plasmanyl (O-) and plasmalogens (P-)– for specific carbon chain lengths and degree of unsaturation (*e.g.*, P-14:0 and O-14:1), which made impossible to distinguish between P- and O- based on their backbones, and (ii) the low fragment intensity, which was insufficient to determine C═C position. Additionally, the presence of PUFA in the *sn*-2 position, further contributed to spectral complexity.

From the identified GP, the majority of the unsaturated esterified FAC contained from C16 to C22 carbon atoms, with minor amounts of C14, and exhibited an unsaturation degree ranging from 0 to 6 [18]. Based on the position of the first C═C relative to the methyl end of the chain, these unsaturated esterified FAC were classified into ω-series families (*e.g.,* ω-3, ω-6, ω-7, ω-9, ω-10) (Table 1 and Fig. 4). This classification reflected differences in their origins, since lipid species belonging to the ω-7, ω-9 and ω-10 series are known to be endogenously synthesized de *novo*, using saturated FA as precursors (Fig. 4A), whereas ω-3 and ω-6 series are regulated by dietary intake and nutritional supplements, requiring the intake of two essential FA precursors, α-linolenic acid (ALA) and linoleic acid (LA) [28] (Fig. 4B).

Among the 120 structurally elucidated unsaturated GP, 79 contained at least one esterified FAC (*sn*-1 and/or *sn*-2) from the ω-6 series, making it the most predominant series within this lipid class, followed by the ω-3 series. Within the ω-9, oleic acid (OA) –FA(18:1(n-9))– was predominant (Supplemental Fig. S9A), recognized for its role in maintaining membrane integrity and supporting cellular function [29]. The ω-7 series was less represented, with only few GP containing palmitoleic acid –FA(16:1(n-7))– and vaccenic acid –FA(18:1(n-7))–, both synthesized from palmitic acid (Table 1, Fig. 4A and Supplemental Table S6). Although ω-7 FA have been associated to metabolic regulation and anti-inflammatory effects [30], their functions remain less understood compared to the widely studied ω-3 and ω-6 series.

Of all esterified FAC characterized, the most prevalent were arachidonic acid (AA) –FA(20:4(n-6))–, followed by LA –FA(18:2(n-6))–, and cervonic acid (DHA) –FA(22:6(n-3))–, as they frequently occupy the *sn*-2 position of almost all PC series (Supplemental Fig. S9A). AA and LA, both key members of the ω-6 series, play critical roles in membrane structure and numerous physiological functions. DHA, the most abundant ω-3 FA identified, is essential in maintaining neuronal and retinal membrane integrity, supporting cognitive performance and visual function [31]. Functionally, ω-6 and ω-3 esterified FAC are transformed by phospholipase A_2 into free FA, serving as ligands for different cyclooxygenases and lipoxygenases, and producing highly active pro-inflammatory eicosanoids in the case of ω-6 FA, and less potent anti-inflammatory eicosanoids for ω-3 FA [32] (Supplemental Fig. S10).

In addition, the C═C position within the esterified FAC of unsaturated SM was also determined, as the sphingoid base backbone consistently maintains C═C positions, regardless of the lipid species. Inspection of the EIEIO-MS/MS spectra identified C═C positions in 6 SM, accounting for 50 % of those with an unsaturated esterified FAC reported in our database [18]. These FAC contained from C14 to C24 carbon atoms and 0–2 degrees of unsaturation [18]. Identified FAC included OA –FA(18:1(n-9))–, gondoic acid –FA(20:1(n-9))–, erucic acid –FA(22:1(n-9))–, nervonic acid –FA(24:1(n-9))– and tetracosadienoic

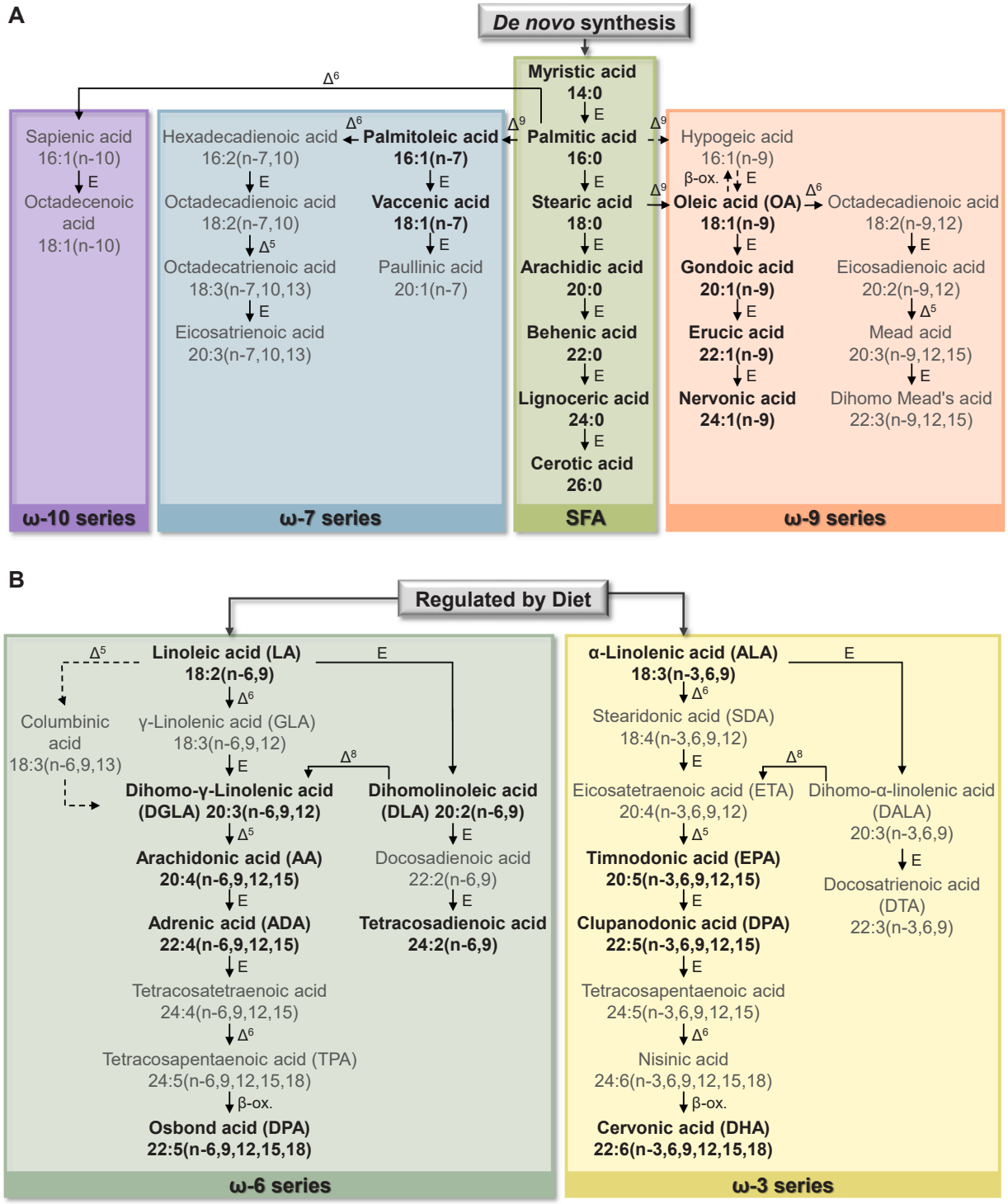

Fig. 4. Fatty acid synthesis in mammals. (A) Fatty acids derived from ω-7, ω-9 and ω-10 series, endogenously synthesized *de novo* from the corresponding saturated FA. (B) Fatty acids derived from ω-3 and ω-6 series regulated from dietary intake. FA highlighted in bold are the ones detected in this analysis. E = *elongase*; Δ = *desaturase*; β-ox. = β-oxidation.

acid –FA(24:2(n-6,9))–, with all except the latter belonging to the ω-9 series (Table 1 and Fig. 4). Among all, OA, gondoic acid and erucic acid were predominant and consistently found across all sphingoid base backbone series (d18:0, d18:1 and d18:2) (Supplemental Fig. S9B), contributing to membrane stability and signaling, and underscoring their importance in maintaining cellular structural integrity [33]

As a result, our SRM 1950 LC-MS lipidomic database has been updated to include annotations up to the C=C position of the identified lipid species (Supplemental Table S7).

To further refine structural details, an initial attempt was made to assess the *cis/trans* isomerism using authentic endogenous lipid standards. The configuration was evaluated by analyzing the intensity ratio of fragments generated at the C-C bonds adjacent to the C=C, as previously described by Baba et al. [10]. Following this approach, in the *cis* configuration, the radical fragment at the single bond preceding the C=C shows higher intensity than the hydrogen-loss (-H) non-radical

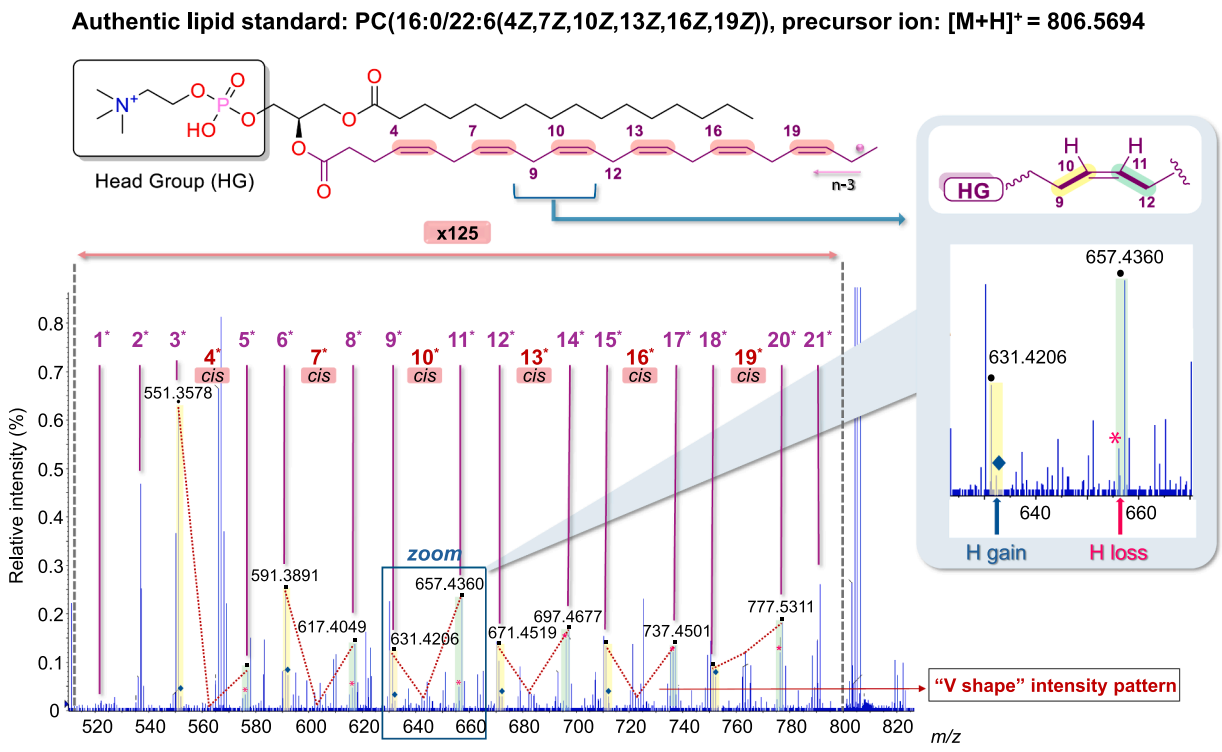

Fig. 5. Evaluation of *cis* configuration in the *sn*-2 FAC present in the authentic lipid standard PC(16:0/22:6(4*Z*,7*Z*,10*Z*,13*Z*,16*Z*,19*Z*)) using ESI(+)-EIEIO-MS/MS. The spectrum was amplified 125-fold to evaluate the fragmentation intensity pattern at the C-C bonds adjacent the C═C [10]. Differences in the intensity ratio of the fragments were observed both before and after the C═C. In *cis* configuration, at the single bond prior the C═C (highlighted in green), the radical fragment (denoted by a black dot •) has a higher intensity than the hydrogen-loss (-H) species non-radical fragment (denoted by a pink asterisk *). At the single bond after the C═C (highlighted in yellow), the radical fragment presents a higher intensity than the hydrogen-gain (+H) non-radical fragment (denoted by a blue diamond ◆).

fragment. In contrast, for the *trans* configuration, this order is reversed, with the hydrogen-loss non-radical fragment exhibiting greater intensity than the radical fragment. At the single bond after the C═C, the *cis* configuration displays a higher intensity of the radical fragment compared to the hydrogen-gain (+H) non-radical fragment, while similar intensities are observed for both fragments in the *trans* configuration. Among all standards, full geometric resolution was achieved in PC(16:0/22:6(4*Z*,7*Z*,10*Z*,13*Z*,16*Z*,19*Z*)), confirming *cis* configuration (Fig. 5). Partial geometry assignments were achieved for an additional four standards, which consistently showed *cis* configurations. However, several standards did not yield sufficient diagnostic fragments to resolve geometry.

Within SRM 1950, geometry was confidently annotated in 7 GP (5.8 % of all GP annotated with C═C positions), all of which displayed *cis* configurations (Supplemental Fig. S11). While these results suggest a predominance of *cis* isomers in the plasma reference material, consistent with the activity of fatty acid desaturase enzymes in mammalian lipid biosynthesis [34], further analysis under optimized conditions are required to robustly distinguish *cis*/*trans* isomers in complex lipid mixtures, due to the limited scope of the current method.

Considering all this information, and despite the strengths of EIEIO-MS/MS for C═C position determination, certain limitations persist. The technique is restricted to lipid species that ionize in ESI(+), meaning those that do not ionize in this polarity require charge-switching derivatization strategies. Structural elucidation of certain lipid subclasses, such as cholesteryl esters, also proves difficult due to insufficient eKE for efficient fragmentation. Additionally, low-abundance lipids require longer accumulation times or targeted inclusion lists to enhance signal intensities. Finally, no db-positional isomers were observed in this analysis, likely due to predominant isomer detection, highlighting the need for improved experimental conditions to enable their resolution.

3.2. Advancements in instrument performance enhances annotation confidence level of lipid species using ESI(+/–)-CID-MS/MS

Given their low-abundance, certain lipid species were characterized only at the sum composition in our lipid database [18]. Therefore, to enhance their annotation confidence level, additional analyses were conducted using ESI(+/–)-CID-MS/MS, which, in combination with the Zeno trap, provided increased sensitivity. CID generated lipid class-specific fragments in ESI(+) and FAC fragments in ESI(–), along with the corresponding precursor ions in both polarities (Supplemental Fig. S12) [24]. However, besides the fragmentation mode and despite their higher efficiency, traditional TOF instruments usually produce ion loss with each pulse between the collision cell and the TOF accelerator, hindering annotation of certain lipid species usually present at lower concentrations in the sample [35]. As an improvement, the SCIEX ZenoTOF 7600 system overcomes this limitation with the Zeno trap [19], which accumulates fragment ions at the exit of the collision cell, then releasing them in reverse mass order towards the accelerator (Supplemental Fig. S12). This approach prevents ion loss and results in significant improvements in MS/MS sensitivity [19,35], particularly enhancing the detection of low *m/z* fragments.

As a result, we successfully identified the FAC and *sn*-position of 29 lipid species, including GP –4 PC, 11 PC (O/P), 2 PE, 1 PE (O/P), 1 PI–, and 10 SM, all reported as sum composition in our database (Supplemental Table S8). In addition, the *sn*-position of 21 GP –1 LPC, 10 PC, 6 PC (O/P) and 4 PE–, previously identified with the FAC but without regioisomerism, were determined (Supplemental Table S8). ESI (–)-CID spectra were mainly used for FAC and *sn*-position determination, except for SM where ESI(+) spectra were inspected to determine the SM backbone. These results demonstrated the capability of the Zeno trap for a more sensitive and comprehensive acquisition, leading to higher-quality MS/MS spectra and enabling the identification up to FAC and

regioisomerism of lower-abundant lipid species in SRM 1950.

3.3. Analytical performance of EIEO versus CID in lipid characterization

When comparing EIEIO *vs* CID fragmentation modes conducted without prior derivatization strategies, clear differences were observed in (i) the type and depth of structural information obtained, (ii) fragmentation efficiency and, (iii) fragmentation patterns. Notably, EIEIO delivered a significantly greater amount of structural data in a single ESI (+) experiment, outperforming the combined results obtained from ESI (+/–)-CID. Specifically, whereas CID requires separate polarity analysis to determine head group identity, FAC composition, and *sn*-positional isomerism, EIEIO enabled the direct and simultaneous elucidation of head group lipid subclass, molecular backbone, FAC identity, *sn*-regioisomerism, and precise C=C position, all within a single experiment conducted in ESI(+). Regarding fragmentation efficiency, EIEIO showed significantly lower performance, resulting in a larger fraction of unfragmented precursor ion and lower overall fragment intensities (Fig. 3 and Supplemental Figs. S5, S6 and S8), occasionally limiting structural elucidation. To address this, accumulation time in the Zeno trap was considerably increased in EIEIO compared to CID (Supplemental Fig. S2), however, in certain cases it remained insufficient for accurate C=C position determination. Finally, for fragmentation patterns EIEIO was found to generate distinct fragmentation profiles based on the identity of the precursor adduct ion (*e.g.*, $[M+H]^+$, $[M+NH_4]^+$, $[M+Na]^+$), whereas CID consistently produced the same fragmentation pattern regardless of the adduct type [13,14,27].

4. Conclusions

In this work, we provide the first comprehensive structural elucidation up to C=C position of unsaturated GP and SM in the SRM 1950 human plasma reference material. Using EIEIO-MS/MS in combination with the enhanced sensitivity of the Zeno trap, we achieved detailed molecular characterization of 120 GP and 6 SM species in a single ESI(+) experiment. Complementary, ESI(+/–)-CID-MS/MS analyses further resolved FAC composition and/or *sn*-positional regioisomer of 59 additional lipid species, improving overall annotation confidence [18].

This in-depth characterization underscores the functional relevance of C=C position on lipid functionality, with ω-3 and ω-6 series, predominant in plasma GP, implicated in inflammatory regulation, and ω-9 lipids, mainly found in SM, contributing to cellular membrane stability. Importantly, although SRM 1950 has been used in previous lipidomic studies, extensive C=C positional information of esterified lipids has not been reported. Therefore, our study fills this gap by generating a curated dataset that extends the structural resolution of SRM 1950, supporting its value as a reference resource for lipidomics.

While these findings should be interpreted within the context of this standard material, they serve as a critical step toward enabling future investigations exploring structure-function relationship in complex biological matrices.

CRediT authorship contribution statement

Sara Martínez: Writing – original draft, Methodology, Investigation, Data curation, Conceptualization, Formal analysis. **Ana Gradillas:** Writing – review & editing, Writing – original draft, Investigation, Data curation, Conceptualization. **Hana Cermakova:** Investigation, Data curation. **Michael Witting:** Writing – review & editing, Methodology, Investigation, Funding acquisition, Conceptualization. **Coral Barbas:** Writing – review & editing, Supervision, Funding acquisition, Conceptualization.

Funding

This research was funded by the Ministry of Science and Innovation of Spain (MICINN), the European Regional Development Fund FEDER, grant number PID2021-122490NB-I00 and La Caixa Foundation, grant number HR24-00686.

Declaration of Competing Interest

The authors declare that they have no known competing financial interests or personal relationships that could have appeared to influence the work reported in this paper.

Acknowledgements and additional information

S.M. acknowledges her predoctoral fellowship from CEINDO (CEU International Doctoral School) and Banco Santander with reference FPI19/06206. In addition, S.M acknowledges the possibility of doing the pre-doctoral mobility to the COST Action Pan-European Network in Lipidomics and EpiLipidomics (EpiLipidNET), CA19105, for the Short-Term Scientific Mission grant (STSM) and CEINDO (CEU International Doctoral School) and Banco Santander for the fellowship for international pre-doctoral mobilities. English revision and proofreading were carried out by Tomás Clive Barker-Tejeda.

Associated content

The following Supporting Information is available free of charge: Supporting Information (pdf) containing Supplemental Figures S1-S12. Supplemental Tables S1-S8 are available as independent Excel files (. xlsx)

Appendix A. Supporting information

Supplementary data associated with this article can be found in the online version at doi:10.1016/j.jpba.2025.117081.

References

[1] Z. Wang, T. Yang, J.Thomas Brenna, D.Hao Wang, Fatty acid isomerism: analysis and selected biological functions, Food Funct. 15 (2024) 1071–1088, https://doi.org/10.1039/D3FO03716A.
[2] H. Martinez-Seara, T. Róg, M. Pasenkiewicz-Gierula, I. Vattulainen, M. Karttunen, R. Reigada, Interplay of unsaturated phospholipids and cholesterol in membranes: effect of the double-bond position, Biophys. J. 95 (2008) 3295–3305, https://doi.org/10.1529/biophysj.108.138123.
[3] J.R. Bonney, B.M. Prentice, Perspective on emerging mass spectrometry technologies for comprehensive lipid structural elucidation, Anal. Chem. 93 (2021) 6311–6322, https://doi.org/10.1021/acs.analchem.1c00061.
[4] M. Fabritius, B. Yang, Analysis of triacylglycerol and phospholipid sn-positional isomers by liquid chromatographic and mass spectrometric methodologies, Mass Spectrom. Rev. 37279164 (2023), https://doi.org/10.1002/mas.21853.
[5] T. Cajka, O. Fiehn, Comprehensive analysis of lipids in biological systems by liquid chromatography-mass spectrometry, Trends Anal. Chem. 61 (2014) 192–206, https://doi.org/10.1016/j.trac.2014.04.017.
[6] S. Heiles, Advanced tandem mass spectrometry in metabolomics and lipidomics-methods and applications, Anal. Bioanal. Chem. 413 (2021) 5927–5948, https://doi.org/10.1007/s00216-021-03425-1.
[7] W. Zhang, R. Jian, J. Zhao, Y. Liu, Y. Xia, Deep-lipidotyping by mass spectrometry: recent technical advances and applications, J. Lipid Res. 63 (2022) 100219, https://doi.org/10.1016/j.jlr.2022.100219.
[8] D. Wang, H. Xiao, X. Lv, H. Chen, F. Wei, Mass spectrometry based on chemical derivatization has brought novel discoveries to lipidomics: a comprehensive review, Crit. Rev. Anal. Chem. 55 (2025) 21–52, https://doi.org/10.1080/10408347.2023.2261130.
[9] J.W. Jones, C.J. Thompson, C.L. Carter, M.A. Kane, Electron-induced dissociation (EID) for structure characterization of glycerophosphatidylcholine: determination of double-bond positions and localization of acyl chains, J. Mass Spectrom. 50 (2015) 1327–1339, https://doi.org/10.1002/jms.3698.
[10] T. Baba, J.L. Campbell, J.C.Y. Le Blanc, P.R.S. Baker, Distinguishing cis and trans isomers in intact complex lipids using electron impact excitation of ions from organics mass spectrometry, Anal. Chem. 89 (2017) 7307–7315, https://doi.org/10.1021/acs.analchem.6b04734.
[11] J.L. Campbell, T. Baba, Near-complete structural characterization of phosphatidylcholines using electron impact excitation of ions from organics, Anal. Chem. 87 (2015) 5837–5845, https://doi.org/10.1021/acs.analchem.5b01460.
[12] T. Baba, J.L. Campbell, J.C.Y.L. Blanc, P.R.S. Baker, In-depth sphingomyelin characterization using electron impact excitation of ions from organics and mass

spectrometry, J. Lipid Res. 57 (2016) 858–867, https://doi.org/10.1194/jlr.M067199.
[13] T. Baba, J.L. Campbell, J.C.Y. Le Blanc, P.R.S. Baker, Structural identification of triacylglycerol isomers using electron impact excitation of ions from organics (EIEIO), J. Lipid Res. 57 (2016) 2015–2027, https://doi.org/10.1194/jlr.M070177.
[14] T. Baba, J.L. Campbell, J.C.Y. Le Blanc, P.R.S. Baker, K. Ikeda, Quantitative structural multiclass lipidomics using differential mobility: electron impact excitation of ions from organics (EIEIO) mass spectrometry, J. Lipid Res. 59 (2018) 910–919, https://doi.org/10.1194/jlr.D083261.
[15] C. Zhang, X. Xu, S. Zhang, M. Xiao, Y. Liu, J. Li, G. Du, X. Lv, J. Chen, L. Liu, Detection and analysis of triacylglycerol regioisomers via electron activated dissociation (EAD) tandem mass spectrometry, Talanta 270 (2024) 125552, https://doi.org/10.1016/j.talanta.2023.125552.
[16] Y. Chen, J. Yang, X. Wang, Y. Zhang, Y. Shao, H. Li, X. Dong, F. Jiang, C. Hu, G. Xu, Structural annotation method for locating sn- and C=C positions of lipids using liquid chromatography–electron impact excitation of ions from organics (EIEIO)–mass spectrometry, Anal. Chem. 97 (2025) 4998–5007, https://doi.org/10.1021/acs.analchem.4c05560.
[17] H. Takeda, Y. Matsuzawa, M. Takeuchi, M. Takahashi, K. Nishida, T. Harayama, Y. Todoroki, K. Shimizu, N. Sakamoto, T. Oka, M. Maekawa, M.H. Chung, Y. Kurizaki, S. Kiuchi, K. Tokiyoshi, B. Buyantogtokh, M. Kurata, A. Kvasnička, U. Takeda, H. Uchino, M. Hasegawa, J. Miyamoto, K. Tanabe, S. Takeda, T. Mori, R. Kumakubo, T. Tanaka, T. Yoshino, M. Okamoto, H. Takahashi, M. Arita, H. Tsugawa, MS-DIAL 5 multimodal mass spectrometry data mining unveils lipidome complexities, Nat. Commun. 15 (2024) 9903, https://doi.org/10.1038/s41467-024-54137-w.
[18] S. Martínez, M. Fernández-García, S. Londoño-Osorio, A. Gradillas, C. Barbas, Highly reliable LC-MS lipidomics database for efficient human plasma profiling based on NIST SRM 1950, J. Lipid Res. 65 (2024) 100671, https://doi.org/10.1016/j.jlr.2024.100671.
[19] SCIEX, Zeno Trap - Defining new levels of sensitivity without compromise, ⟨https://sciex.com/content/dam/SCIEX/pdf/brochures/zeno-trap-whitepaper.pdf⟩.
[20] A. Villaseñor, I. Garcia-Perez, A. Garcia, J.M. Posma, M. Fernández-López, A. J. Nicholas, N. Modi, E. Holmes, C. Barbas, Breast milk metabolome characterization in a single-phase extraction, multiplatform analytical approach, Anal. Chem. 86 (2014) 8245–8252, https://doi.org/10.1021/ac501853d.
[21] J.A. Kirwan, H. Gika, R.D. Beger, D. Bearden, W.B. Dunn, R. Goodacre, G. Theodoridis, M. Witting, L.-R. Yu, I.D. Wilson, Metabolomics quality assurance and quality control consortium (mQACC), quality assurance and quality control reporting in untargeted metabolic phenotyping: mQACC recommendations for analytical quality management, Metab. Off. J. Metab. Soc. 18 (2022) 70, https://doi.org/10.1007/s11306-022-01926-3.
[22] I. Piédrola, S. Martínez, A. Gradillas, A. Villaseñor, V. Alonso-Herranz, I. Sánchez-Vera, E. Escudero, I.A. Martín-Antoniano, J.F. Varona, A. Ruiz, J.M. Castellano, Ú. Muñoz, M.C. Sádaba, Deficiency in the production of antibodies to lipids correlates with increased lipid metabolism in severe COVID-19 patients, Front. Immunol. 14 (2023) 1188786, https://doi.org/10.3389/fimmu.2023.1188786.
[23] G. Liebisch, E. Fahy, J. Aoki, E.A. Dennis, T. Durand, C.S. Ejsing, M. Fedorova, I. Feussner, W.J. Griffiths, H. Köfeler, A.H. Merrill, R.C. Murphy, V.B. O'Donnell, O. Oskolkova, S. Subramaniam, M.J.O. Wakelam, F. Spener, Update on LIPID MAPS classification, nomenclature, and shorthand notation for MS-derived lipid structures, J. Lipid Res. 61 (2020) 1539–1555, https://doi.org/10.1194/jlr.S120001025.
[24] O. Fiehn, D. Robertson, J. Griffin, M. van der Werf, B. Nikolau, N. Morrison, L. W. Sumner, R. Goodacre, N.W. Hardy, C. Taylor, J. Fostel, B. Kristal, R. Kaddurah-Daouk, P. Mendes, B. van Ommen, J.C. Lindon, S.-A. Sansone, The metabolomics standards initiative (MSI), Metabolomics 3 (2007) 175–178, https://doi.org/10.1007/s11306-007-0070-6.
[25] M. Pearson, C. Hunter, T. ⟨https://sciex.com/tech-notes/life-science-research/lipidomics/complete-structural-elucidation-of-lipids-in-a-single-experiment0⟩.
[26] A. Korf, V. Jeck, R. Schmid, P.O. Helmer, H. Hayen, Lipid species annotation at double bond position level with custom databases by extension of the MZmine 2 open-source software package, Anal. Chem. 91 (2019) 5098–5105, https://doi.org/10.1021/acs.analchem.8b05493.
[27] X. Wang, X. Sun, F. Wang, C. Wei, F. Zheng, X. Zhang, X. Zhao, C. Zhao, X. Lu, G. Xu, Enhancing metabolome annotation by electron impact excitation of ions from organics-molecular networking, Anal. Chem. 96 (2024) 1444–1453, https://doi.org/10.1021/acs.analchem.3c03443.
[28] R.K. Saini, Y.-S. Keum, Omega-3 and omega-6 polyunsaturated fatty acids: dietary sources, metabolism, and significance - A review, Life Sci. 203 (2018) 255–267, https://doi.org/10.1016/j.lfs.2018.04.049.
[29] H. Sales-Campos, P.R. de Souza, B.C. Peghini, J.S. da Silva, C.R. Cardoso, An overview of the modulatory effects of oleic acid in health and disease, Mini Rev. Med. Chem. 13 (2013) 201–210, https://doi.org/10.2174/1389557511313020003.
[30] N.L. Weir, B.T. Steffen, W. Guan, L.M. Johnson, L. Djousse, K.J. Mukamal, M. Y. Tsai, Circulating omega-7 fatty acids are differentially related to metabolic dysfunction and incident type II diabetes: the multi-ethnic study of atherosclerosis (MESA), Diabetes Metab. 46 (2020) 319–325, https://doi.org/10.1016/j.diabet.2019.10.005.
[31] N.G. Bazan, M.F. Molina, W.C. Gordon, Docosahexaenoic acid signalolipidomics in nutrition: significance in aging, neuroinflammation, macular degeneration, Alzheimer's, and other neurodegenerative diseases, Annu. Rev. Nutr. 31 (2011) 321–351, https://doi.org/10.1146/annurev.nutr.012809.104635.
[32] M.M. Papamichael, C. Katsardis, D. Tsoukalas, C. Itsiopoulos, B. Erbas, Plasma lipid biomarkers in relation to BMI, lung function, and airway inflammation in pediatric asthma, Metab. Off. J. Metab. Soc. 17 (2021) 63, https://doi.org/10.1007/s11306-021-01811-5.
[33] M.T. Nakamura, T.Y. Nara, Structure, function, and dietary regulation of Δ6, Δ5, and Δ9 desaturases, Annu. Rev. Nutr. 24 (2004) 345–376, https://doi.org/10.1146/annurev.nutr.24.121803.063211.
[34] J.M. Lee, H. Lee, S. Kang, W.J. Park, Fatty acid desaturases, polyunsaturated fatty acid regulation, and biotechnological advances, Nutrients 8 (2016) 23, https://doi.org/10.3390/nu8010023.
[35] SCIEX, Qualitative flexibility combined with quantitative power - using the ZenoTOF 7600 system, powered by SCIEX OS Software, ⟨https://sciex.com/tech-notes/technology/qualitative-flexibility-combined-with-quantitative-power—using⟩.